Journal of Quantitative Spectroscopy & Radiative Transfer 346 (2025) 109620

Contents lists available at ScienceDirect

Journal of Quantitative Spectroscopy and Radiative Transfer

journal homepage: www.elsevier.com/locate/jqsrt

Updated ro-vibrational MARVEL levels for ammonia $^{14}NH_3$

Oleksiy A. Smola, Sergei N. Yurchenko *, Jonathan Tennyson

Department of Physics and Astronomy, University College London, London, WC1E 6BT, UK

ARTICLE INFO

Keywords:
Rovibrational energy levels
NH3
Ammonia
Line positions
Transitions
MARVEL

ABSTRACT

An extended list of empirical ro-vibrational energy levels for the ammonia isotopologue $^{14}NH_3$ is constructed using the MARVEL procedure. The final transition set includes 69710 experimental line positions from 97 experimental sources covering the wavenumber range below 18177 cm^{-1} and rotational excitations up to $J = 29$. The transition set incorporates 23844 newly collated experimental transitions extending the covered energy range beyond 7500 cm^{-1}, yielding 10753 empirical energy levels with uncertainties, an increase of 5817 from the previous MARVEL study. This MARVEL set is then used to reMARVELise the CoYuTe line list for $^{14}NH_3$, yielding a total of 641836 experimentally accurate line positions. The updated line list is available from www.exomol.com.

1. Introduction

Ammonia, NH_3, is one of the first polyatomic molecules to be detected in the interstellar medium [1,2]. Since then, the rich ammonia spectrum, along with its high abundance, has made it a useful probe of physical and chemical conditions of molecular clouds [3–7]. In our solar system, ammonia has been detected in the atmospheres of Jupiter and Saturn [8–13], where features around 647 nm in particular are used in determining the ammonia abundance and to probe cloud top pressures [14]. Ammonia has recently been firmly detected in an exoplanet atmosphere [15] following more tentative detections [16,17]. Its role as a potential biosignature in the atmospheres exoplanets has also been discussed [18]. The presence of ammonia is also thought to be a key indicator of cool Y dwarfs [19,20].

On Earth, ammonia is vital for agriculture, since it serves as a key component in the production of many fertilizers [21]. The resulting release of ammonia into the surrounding environment is known to disrupt the nitrogen cycle, potentially endangering dependent ecosystems [22, 23]. Consequently, pollution of ammonia and other nitrogen-bearing species in the atmosphere needs to be monitored [24,25]. In particular, oxidation of atmospheric ammonia leads to the production N_2O [26], a prominent greenhouse gas [27].

The experimental spectroscopy of ammonia spans well over a century with the first known recorded spectra attributed to Eder [28, 29] in the 19th century. The inversion splitting was subsequently measured in the infrared [30] and far-infrared regions [31,32]. Such inversion transitions make ammonia a particularly potent microwave amplifier, a property which was exploited in the development of the first maser [33].

For theoretical computations, ammonia has served as a molecule of interest to test methods that can describe large amplitude motions. In the case of ammonia, the relevant large amplitude motion is the so-called umbrella motion. Extensive efforts have been made to compute accurate ro-vibrational energies and transition frequencies of ammonia [34–39]. In recent years, accurate *ab initio* surfaces have been computed [40,41] for the full six-dimensional potential energy surface of ammonia using MRCI and coupled-cluster methods, respectively. The former surface was subsequently refined to empirical energy levels [42] determined by the MARVEL (Measured Active Rotational Vibrational Energy Levels) procedure [43] during the production of the highly accurate variationally computed CoYuTe line list [44]. The CoYuTe line list was also MARVELised, meaning variationally computed levels were substituted for empirical energies where available, making the line list suitable for high-resolution studies.

The MARVEL procedure has been applied to a range of diatomic [45–49] and polyatomic molecules [50–55]; $^{14}NH_3$ itself has been the subject of two previous MARVEL studies [42,56], together comprising experimental transitions from 83 sources [57–140]. More recently, the $^{15}NH_3$ isotopologue has also been subjected to a MARVEL treatment [141]. Although Furtenbacher et al. [42] updated the transition set obtained by Al Derzi et al. [56], it excluded transitions above 7500 cm^{-1}, meaning some of the then available spectroscopic literature [64,142–144] was not incorporated into the study, one of which [64] was included in Al Derzi et al. [56]. Here we update the existing transition sets compiled in the past two studies [42,56] with newly assigned, measured and remeasured transitions from 14 new sources [142–155], which significantly improve the coverage of

* Corresponding author.
E-mail addresses: s.yurchenko@ucl.ac.uk (S.N. Yurchenko), j.tennyson@ucl.ac.uk (J. Tennyson).

https://doi.org/10.1016/j.jqsrt.2025.109620
Received 30 June 2025; Received in revised form 31 July 2025; Accepted 2 August 2025
Available online 11 August 2025

the near infrared region. In part these improvements have been made possible by the use of the MARVELised CoYuTe line list to assign spectra of $^{14}NH_3$ in this region.

2. Method

2.1. MARVEL procedure

The MARVEL procedure is based on the theory of spectroscopic networks, and facilitates the derivation of empirical energy levels from networks of experimentally measured transition frequencies, while ensuring that each derived level is accompanied by statistically sound uncertainties. The interested reader may find more details on the MARVEL procedure, and spectroscopic network theory in Furtenbacher et al. [43], Tobias et al. [156] and Arendas et al. [157,158]. Application of the MARVEL procedure requires collating available spectroscopic transition frequencies, accompanied by their uncertainties, quantum number labels for the upper, and lower states and a segment tag denoting the literature source for each transition. For uncertainty propagation, we apply the bootstrapping algorithm available in MARVEL 4.1 [159].

2.2. Quantum numbers

Three-fold symmetric ammonia isotopologues belong to the D_{3v}(M) molecular symmetry group [160], encompassing the irreducible representations $\Gamma = A_1'$, A_2', E', A_1'', A_2'', or E'', which define the symmetry selection rules $A_1' \leftrightarrow A_1''$, $A_2' \leftrightarrow A_2''$, and $E' \leftrightarrow E''$. In the case of $^{14}NH_3$, the nuclear spin statistical weights are $g_{ns}^{A_1} = 0$, $g_{ns}^{A_2} = 12$ and $g_{ns}^{E} = 6$ [160], meaning that no levels belonging to the irreps A_1' or A_1'' exist in nature, including the theoretical ro-vibrational ground state ($J = 0$ and $\Gamma = A_1'$).$^{14}NH_3$ possesses six vibrational degrees of freedom: a symmetric hydrogen stretch v_1, the inversion mode v_2, the asymmetric stretch v_3, the bending motion v_4, and the vibrational angular momenta associated with the latter two excitations l_3 and l_4, respectively. Ammonia is a symmetric top, with rotational quantum numbers J and K to denote total rotational angular momentum and the projection along the axis with the highest moment of inertia, respectively. Additionally, due to the inversion tunnelling motion between the two minima of the potential, ammonia states also split into symmetric "s" and antisymmetric "a" components. The first MARVEL study on $^{14}NH_3$ [56] adopted the quantum numbers (v_1, v_2, v_3, v_4, l_3, l_4, J, K, i, Γ_r, Γ_v, Γ_{tot}) [161], where i, Γ_r, Γ_v and Γ_{tot} denote the inversion, rotational, vibrational and total symmetry respectively. The second MARVEL set [42], instead used $L_3 = |l_3|$ and $L_4 = |l_4|$ for the vibrational angular momenta, and dropped the individual symmetry components Γ_r and Γ_v. The block number N_b, denoting the energy ordering of a state within a TROVE (Theoretical ROVibrational Energies) [162] computed ro-vibrational $J - \Gamma_{tot}$ block, was also introduced. The final set of quantum numbers used by Furtenbacher et al. [42] was then (v_1, v_2, v_3, v_4, L_3, L_4, J, K, i, Γ_{tot}, N_b) which we retain in this study. The MARVEL study on the $^{15}NH_3$ isotopologue [141] made use of a vibrational index instead of the block number. Both the block number and vibrational index depend on the variational model used to compute energies and as such should not be treated as rigorous.

We follow the HITRAN convention for the zero-point-energy and set the lowest measured state to zero, which in the case of $^{14}NH_3$ is $J = 0$, $K = 0$, a, A_2'' (0,0,0^0,0^0), i.e. the upper, asymmetric inversion component of the ground state, with the symmetric component $J = 0$, $K = 0$, s, A_1' (0,0,0^0,0^0) being forbidden due to the nuclear spin statistics. The inversion splitting separating the two states is 0.793399 cm^{-1}, as determined by Urban et al. [125]. The previous two MARVEL studies of $^{14}NH_3$ used a different convention of setting the absolute zero to the theoretical, non-existent, ground state of $J = 0$, $K = 0$, s, A_1' (0,0,0^0,0^0), which we now modify such that the MARVEL standard is now consistent with that of HITRAN. See also the recent MARVEL data set of $^{15}NH_3$ [141] where the same definition was used.

3. Experimental data

In addition to the transitions from the previous MARVEL datasets, Al Derzi et al. [56] and Furtenbacher et al. [42], we consider a total of 14 additional sources [142–155], consisting of newly assigned experimental transitions, as well as assigned transitions for which the uncertainties in the transition frequencies have been redetermined. We also consider an older source [64] of transitions in the visible region, which was included in Al Derzi et al. [56] but omitted in Furtenbacher et al. [42]. A summary of the sources considered, their spectral coverage and uncertainties are given in Table 1. In total, there are 69 710 validated transitions, an increase of 23 673 from Furtenbacher et al. [42]. No new empirical determination has been made for the separation between the forbidden A_1' ground state with the *ortho* (A_2', A_2'') and *para* (E', E'') networks, so the so-called magic numbers derived by Urban et al. [125] that were used previously [42] are retained. Two newer experimental sources [163,164] were neglected as the transition sets lack the quantum number assignments required for the MARVEL procedure. The complete transition set, as well as lists of invalidated and reassigned lines are available as part of the supplementary data.

3.1. Source specific comments

86CoLe [64] reported transitions which were found to possess systematic discrepancies of around 0.04 cm^{-1} from those of 18ZoKoOv [144]. 86CoLe assignments only included rotational quantum numbers. In Al Derzi et al. [56] transitions from 86CoLe were given ad-hoc vibrational assignments using the BYTe line list [39]. Here, if a given 86CoLe line has a corresponding line in 18ZoKoOv, we adopt the latter assignment. Otherwise, the vibrational quantum numbers are taken from CoYuTe [44], which while remaining ad-hoc, should provide a slightly more realistic determination of the vibrational quanta than the less accurate BYTe model.

The sources 22CaCeVaCa [151], 22CaCeVaCaa [152], 21CeCaCo [148], 21CaCeBeCa [149] and 23CaCeVo [153] adopted the quantum numbers previously used by Furtenbacher et al. [42] for their assignment. This helped reduce the effort required for integrating these sources into the established dataset. Some assigned ro-vibrational levels had already been observed but were assigned different vibrational quantum numbers while having the same block number. Therefore, a number of lines had to be reassigned to make them consistent with the previously assigned data.

22HuSuTo [150] contained 35 line assignments that break symmetry selection rules, resulting in their invalidation.

16BaYuTeBe [142], 17BaPoYuTe [143], 18ZoKoOv [144] and 21ZoBeVaCi [147] extend beyond the 7500 cm^{-1} cut-off applied in the previous MARVEL study. Experimental quantum number assignments are given without the TROVE block number N_b. The block numbers are given ad-hoc assignments based on the closest match to variational CoYuTe levels [44] within the same $J - \Gamma_{tot}$ block. Degeneracies in the block number were manually resolved.

19SvRaVo [146] offers 5 new assignments or reassignments of previous lines, as of the time of the HITRAN 2016 release [165], all but one are invalidated. The one validated new assignment was found to already be present in the previous MARVEL study [42]. The other invalidated lines correspond to those where the rotational assignment was incomplete.

4. Results

Applying the MARVEL procedure to the transition set yields a total of 10 753 empirically determined energy levels, increased from the 4936 levels derived by Furtenbacher et al. [42]. The derived energy levels as a function of the rotational quantum number J are given in Fig. 1. The corresponding uncertainties for the new energy levels,

Table 1
Sources of the MARVEL transition set, their spectral range, number of validated transitions V out of the total T, average uncertainty AU and sorted by median uncertainty MU. Sources highlighted in bold are newly considered in this work.

Source tag	Citation	*Range* (cm^{-1})	V/T	AU	MU
09CaDoPu	[57]	19.10–19.10	2/2	6.5×10^{-9}	6.5×10^{-9}
70KuWo	[58]	0.72–0.82	5/5	7.0×10^{-9}	7.0×10^{-9}
67Kukolich	[59]	0.79–0.80	3/3	7.0×10^{-9}	7.0×10^{-9}
65Kukolich	[60]	0.76–0.76	1/1	1.7×10^{-8}	1.7×10^{-8}
75PoKa	[61]	0.24–1.33	119/119	2.6×10^{-7}	1.7×10^{-7}
74CoPo	[62]	0.69–1.96	50/50	2.9×10^{-7}	1.7×10^{-7}
80SiSm	[63]	0.18–0.41	15/15	3.3×10^{-7}	3.3×10^{-7}
88TaEnHi	[69]	10.67–11.08	14/14	1.1×10^{-6}	5.3×10^{-7}
82SaHaAmSh	[65]	2.28–5.93	11/12	6.7×10^{-7}	6.7×10^{-7}
16TwHaSe	[67]	6487.84–6636.72	56/58	8.3×10^{-7}	6.7×10^{-7}
96WiBeKlUr	[66]	38.98–40.54	3/3	6.7×10^{-7}	6.7×10^{-7}
98FiKhRuLe	[68]	967.25–967.25	1/1	8.7×10^{-7}	8.7×10^{-7}
90SmFiDa	[70]	0.34–1.54	14/14	1.6×10^{-6}	1.3×10^{-6}
10YuPeDrSu	[75]	13.33–157.19	175/175	3.5×10^{-6}	1.7×10^{-6}
92SaEnHiPo	[71]	2.35–1387.92	80/80	2.2×10^{-6}	2.0×10^{-6}
80Cohen	[72]	2.09–4.07	17/17	2.2×10^{-6}	2.3×10^{-6}
11DrYuPeGu	[73]	84.01–89.04	5/5	3.3×10^{-6}	3.3×10^{-6}
84MaScFrKr	[77]	934.38–1075.20	9/9	4.3×10^{-6}	3.3×10^{-6}
11LeTrDaBo	[74]	965.79–965.79	1/1	3.3×10^{-6}	3.3×10^{-6}
08SuLeXu	[76]	1027.03–1075.20	14/14	4.2×10^{-6}	3.3×10^{-6}
06ChPePiMa	[80]	15.55–46.47	30/30	1.1×10^{-5}	3.8×10^{-6}
96KrTrBoBa	[78]	40.52–40.54	2/2	5.3×10^{-6}	5.3×10^{-6}
16PeYuPi	[79]	13.72–90.96	159/159	8.3×10^{-6}	6.7×10^{-6}
98BeUrWi	[82]	4.67–25.45	3/3	1.3×10^{-5}	1.1×10^{-5}
00UrHeKhFi	[81]	948.23–951.78	2/2	1.3×10^{-5}	1.3×10^{-5}
85SiRe	[83]	788.51–1084.63	15/15	2.3×10^{-5}	1.7×10^{-5}
80BeGeKrMa	[84]	4.67–35.79	55/55	4.8×10^{-5}	3.3×10^{-5}
11GuJeMoPe	[85]	1126.03–1171.44	22/22	5.9×10^{-5}	4.0×10^{-5}
82MiToCaLi	[86]	1084.58–1084.62	5/5	7.8×10^{-5}	6.7×10^{-5}
86SaScMaPo	[88]	772.44–1157.39	138/138	1.4×10^{-4}	6.8×10^{-5}
85BrTo	[87]	814.24–1122.05	81/81	8.8×10^{-5}	7.0×10^{-5}
89UrTuRaGu	[89]	3984.94–4648.05	780/785	1.5×10^{-4}	9.0×10^{-5}
24ZhAgSeSh	[155]	1084.58–1084.63	6/6	1.0×10^{-4}	1.0×10^{-4}
83PoMa	[94]	19.10–316.78	204/204	3.5×10^{-4}	1.3×10^{-4}
22CaCeVaCa	[151]	3900.38–4704.02	6038/6052	4.9×10^{-4}	1.3×10^{-4}
77KoMuHiBu	[90]	887.88–971.88	11/11	1.6×10^{-4}	1.4×10^{-4}
83ShBjSc	[93]	891.88–1103.49	88/88	2.6×10^{-4}	2.0×10^{-4}
81SaMiWo	[99]	932.88–1084.63	32/32	4.7×10^{-4}	2.0×10^{-4}
83UrPaKaYa	[96]	709.09–1158.67	640/640	3.9×10^{-4}	2.0×10^{-4}
95FaItYa	[98]	904.80–1178.75	133/133	4.1×10^{-4}	2.0×10^{-4}
19SvRaVo	[146]	6540.25–6866.83	30/46	2.0×10^{-4}	2.0×10^{-4}
81SaWo	[91]	924.95–1043.15	39/39	2.0×10^{-4}	2.0×10^{-4}
84PoMa	[95]	723.27–1250.17	533/533	3.7×10^{-4}	2.0×10^{-4}
92SaEnHiPo_S2	[71]	1388.06–1859.71	727/727	7.7×10^{-4}	2.0×10^{-4}
94ChChCh	[92]	928.56–955.06	48/48	2.4×10^{-4}	2.0×10^{-4}
22CaCeVaCaa	[152]	4706.41–5648.12	6562/6562	5.2×10^{-4}	2.2×10^{-4}
76FrOk	[103]	926.05–1084.61	55/56	6.2×10^{-4}	2.7×10^{-4}
10YuPeDrSu_S2	[75]	39.08–672.64	1600/1600	4.6×10^{-4}	3.0×10^{-4}
23CaCeVo	[153]	5650.51–6349.75	3344/3363	2.4×10^{-3}	3.1×10^{-4}
95KlTaBr	[121]	429.37–3114.85	2061/2066	1.6×10^{-3}	4.0×10^{-4}
79HiJeFa	[97]	949.45–949.45	1/1	4.1×10^{-4}	4.1×10^{-4}
18PeYuPeSu	[111]	16.07–1572.77	1266/1266	1.1×10^{-3}	4.2×10^{-4}
81UrSpPaKa	[110]	4.67–969.02	299/299	1.0×10^{-3}	4.7×10^{-4}
87DCunha	[113]	701.46–1187.35	196/196	1.1×10^{-3}	5.0×10^{-4}
87LeLaGuTa	[107]	1800.00–2099.43	455/455	8.0×10^{-4}	5.0×10^{-4}
89GuAbTuRa	[119]	3023.32–3674.90	1380/1382	1.3×10^{-3}	5.0×10^{-4}
93PiDa	[106]	3331.04–3415.41	100/100	7.1×10^{-4}	5.0×10^{-4}
96BrMa	[104]	4802.17–5292.97	602/615	6.2×10^{-4}	5.0×10^{-4}
99FaYa	[105]	770.91–1178.75	126/126	7.0×10^{-4}	5.0×10^{-4}
84Weber	[108]	1511.31–1880.25	176/176	8.3×10^{-4}	5.0×10^{-4}
00CoKlTaBr	[101]	1333.01–2096.09	1202/1202	5.6×10^{-4}	5.0×10^{-4}
99KlBrTaKo	[112]	2980.45–3633.84	2162/2162	1.1×10^{-3}	5.0×10^{-4}
01CoTaKlBr	[118]	1201.93–2749.22	1305/1305	1.3×10^{-3}	5.0×10^{-4}

(*continued on next page*)

propagated with and without the bootstrapping procedure, are given in Fig. 2. As can be seen, many levels share the same uncertainty, indicating a need for more uniquely determined uncertainties, particularly at higher frequencies. Many of the energy levels are also determined with only one transition frequency, so only one uncertainty is varied at each bootstrap iteration, meaning the difference in uncertainty from applying bootstrapping is minimal.

Residuals between variationally computed CoYuTe levels [44] and the newly determined MARVEL energies are given in Fig. 3. The large residuals in the region beyond 7000 cm^{-1} reflect the lower accuracy of the variational model and the difficulty in assigning quantum numbers at higher frequencies.

Table 1 (*continued*).

77HiKoBuFa	[100]	887.88–1027.03	9/9	5.2×10^{-4}	5.0×10^{-4}
13ArMaBo	[102]	991.69–1859.71	462/462	5.7×10^{-4}	5.0×10^{-4}
14FoGoHeSo	[120]	6410.29–6764.53	209/212	1.5×10^{-3}	5.0×10^{-4}
21CeCaCo	[148]	4275.14–4356.61	701/703	5.3×10^{-4}	5.0×10^{-4}
86UrCuMaRa	[124]	511.37–1347.81	579/579	1.9×10^{-3}	5.8×10^{-4}
16PeYuPi_S2	[79]	39.55–707.26	1221/1221	7.7×10^{-4}	6.0×10^{-4}
84UrCuNaPa	[125]	1167.86–2126.72	949/950	2.0×10^{-3}	6.6×10^{-4}
86PaUrSpRa	[115]	1425.79–1892.23	70/73	1.2×10^{-3}	7.6×10^{-4}
78Nereson	[114]	942.57–956.15	27/27	1.1×10^{-3}	8.1×10^{-4}
94BrPe	[109]	38.98–3415.10	174/174	1.0×10^{-3}	9.1×10^{-4}
16PeYuPi_S3	[79]	61.94–682.28	1469/1470	1.6×10^{-3}	1.0×10^{-3}
14CeHoVeCa	[122]	4275.36–4339.67	222/229	1.7×10^{-3}	1.0×10^{-3}
13DoHiYuTe	[128]	0.43–4810.58	10 654/10 661	2.5×10^{-3}	1.0×10^{-3}
22HuSuTo	[150]	5604.96–6299.58	1556/1602	1.0×10^{-3}	1.0×10^{-3}
12SuBrHuSc	[123]	6346.76–6973.52	1057/1072	1.8×10^{-3}	1.0×10^{-3}
11ZoShOvPo	[127]	779.56–2029.23	5900/5915	2.4×10^{-3}	1.0×10^{-3}
16SuYuPePi	[117]	50.71–657.78	1724/1725	1.2×10^{-3}	1.0×10^{-3}
78Jones	[116]	887.88–1032.13	23/23	1.2×10^{-3}	1.0×10^{-3}
85AnFiFrIl	[126]	3134.65–3620.22	615/615	2.3×10^{-3}	1.4×10^{-3}
23YaSiLa	[154]	2437.76–2457.66	6/6	1.9×10^{-3}	1.7×10^{-3}
86HeBiBa	[129]	620.57–739.44	223/223	2.5×10^{-3}	1.8×10^{-3}
08LeLiXu	[130]	6440.01–6832.30	221/222	2.8×10^{-3}	2.0×10^{-3}
07LiLeXu	[132]	6421.23–6677.99	97/97	3.3×10^{-3}	2.0×10^{-3}
89UrTuRaGu_S2	[89]	3982.84–4633.09	74/74	3.2×10^{-3}	2.6×10^{-3}
21CaCeBeCa	[149]	5651.56–6349.75	1759/1762	3.0×10^{-3}	3.0×10^{-3}
14DiMiQuSc	[131]	3355.01–3355.01	1/1	3.0×10^{-3}	3.0×10^{-3}
80UrSpPaMc	[139]	678.38–2013.99	481/482	7.6×10^{-3}	3.9×10^{-3}
10PeHa	[136]	6460.42–6541.41	16/16	5.8×10^{-3}	5.0×10^{-3}
85UrMiRa	[135]	3148.16–4503.74	478/478	5.7×10^{-3}	5.0×10^{-3}
88SnBa	[133]	931.18–932.14	7/7	5.0×10^{-3}	5.0×10^{-3}
18MaMaMaPa	[145]	1590.87–1633.00	10/10	5.6×10^{-3}	5.0×10^{-3}
71HeDeGo	[134]	19.88–19.88	1/1	5.3×10^{-3}	5.3×10^{-3}
93LuHeNi	[137]	6405.47–6887.90	312/315	6.1×10^{-3}	5.3×10^{-3}
99BePeMe	[138]	6540.24–6624.48	27/27	6.5×10^{-3}	6.1×10^{-3}
16BaYuTeBe	[142]	7403.48–8597.41	2168/2171	1.0×10^{-2}	1.0×10^{-2}
17BaPoYuTe	[143]	9447.15–9895.34	642/642	1.0×10^{-2}	1.0×10^{-2}
15BaYuTeCl	[140]	500.53–1883.66	1347/1366	1.8×10^{-2}	1.4×10^{-2}
89UrTuRaGu_S3	[89]	3969.87–4658.62	32/32	1.8×10^{-2}	1.4×10^{-2}
86CoLe	[64]	15 259.40–15 552.51	319/322	2.0×10^{-2}	2.0×10^{-2}
18ZoKoOv	[144]	15 260.24–18 194.00	309/338	2.7×10^{-2}	2.4×10^{-2}
21ZoBeVaCi	[147]	12 493.81–12 763.49	251/259	4.0×10^{-2}	4.0×10^{-2}

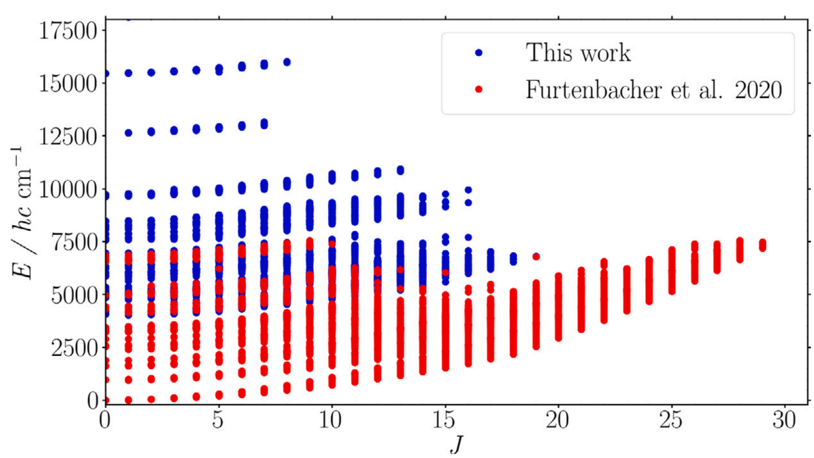

Fig. 1. MARVEL derived energy levels from Furtenbacher et al. [42] and this work as a function of rotational quantum number J.

To be suitable for high-resolution studies, ExoMol line lists are MARVElised, meaning that variationally computed energies and their uncertainties are replaced with the corresponding MARVEL energy and uncertainty values where available [167,168]. The updated list of energy levels is used to once again apply this procedure to the CoYuTe line list [44]. At higher energies some MARVEL levels may be misassigned, or are difficult to match with their variational counterpart due to the reduced accuracy of the spectroscopic model. To minimize the number of potentially problematic levels substituted into the line list, we substitute 8248 of the 10 753 empirical levels, which are chosen such that they are derived from more than one transition, and whose deviation from the variational calculation is no greater than 1 cm^{-1}.

A total of 641 836 experimentally accurate lines are computed from transitions between MARVEL derived levels. To simulate the resulting room temperature spectrum, the ExoCross programme [169] is used, for a temperature of $T = 296$ K, and with the HITRAN intensity cut-off of 10^{-30} cm/molecule applied. With this cut-off, the number of experimentally accurate lines in the spectrum is 396 311. This is to compare to 76 606 $^{14}NH_3$ transitions in HITRAN2020 [170]. Fig. 4 compares the coverage of the MARVELised CoYuTe transitions with

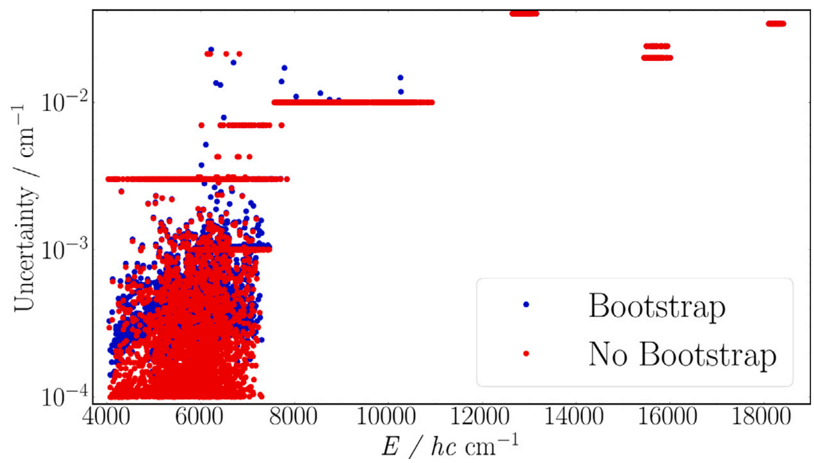

Fig. 2. MARVEL uncertainties of newly derived levels as a function of energy in hc cm^{-1}, with bootstrapping applied for 100 iterations (blue), and with bootstrapping turned off (red).

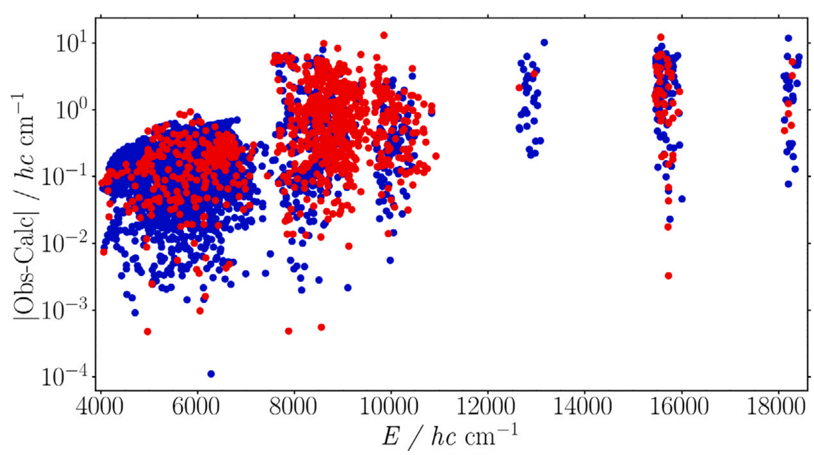

Fig. 3. Absolute Obs-Calc between newly derived MARVEL levels and variationally computed levels in CoYuTe [44]. Levels denoted in red are derived from only a single transition.

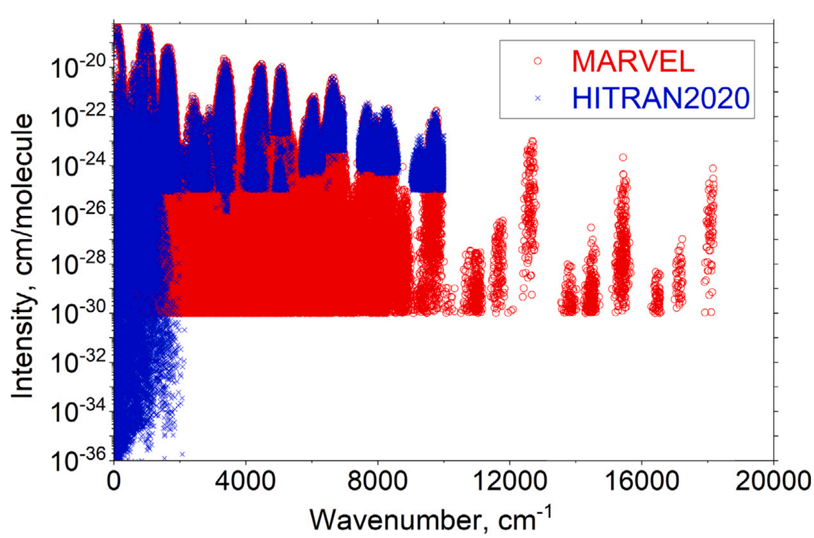

Fig. 4. Comparison of the coverage between HITRAN [166] and MARVEL. For the latter, only transitions with intensities larger than 10^{-30} cm/molecule are shown.

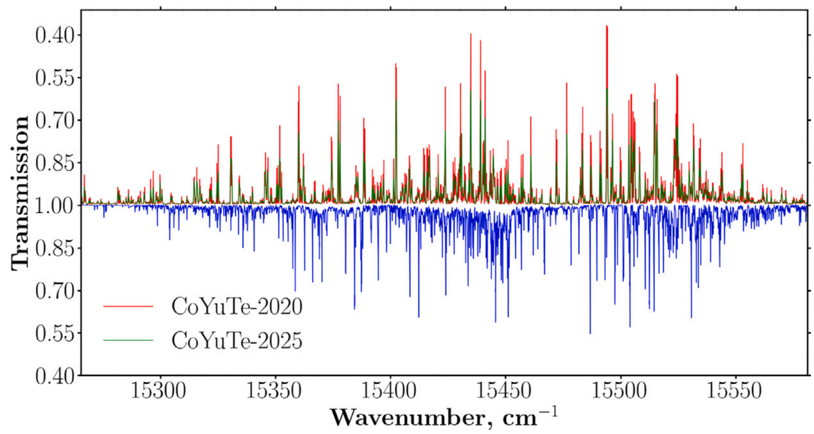

Fig. 5. Comparison of the two MARVELised CoYuTe spectra with that of Giver et al. [171] simulated at $T = 294$ K, digitized by [172]. CoYuTe cross-sections are computed using the ExoCross code [169] with a HWHM = 0.075 cm^{-1} and intensity cutoff = 10^{-40} cm/molecule.

the data coverage in HITRAN2020 by plotting the individual intensities below 18 176 cm^{-1}.

In order to gauge how the newly reMARVELised CoYuTe model performs in the visible region, we compare to the Jupiter spectrum recorded by Giver et al. [171]. Fig. 5 shows the comparison between the 2020 CoYuTe model, the current MARVELised model and Giver's spectrum. The agreement remains similar to that observed by [172]. Line positions remain mostly unchanged, with the most notable difference being decreased intensities in the latest line list.

5. Conclusion

We have applied the MARVEL procedure to derive a further 5817 empirical ro-vibrational energy levels for the ammonia isotopologue $^{14}NH_3$, notably extending the coverage of the MARVEL energy levels list beyond 7500 cm^{-1}. The updated energy level list and reMARVELised CoYuTe line list is expected to be useful as a benchmark for future variational models, and to aid in future assignments, helping to further understanding of the ammonia spectrum. The updated line list is also included as part of the ExoMol database [173–176], intended to aid molecular retrievals of exoplanet atmospheres as well as other astrophysical settings. Although the red spectrum from [144] is included, it remains to be seen as to whether the inclusion of these transitions can aid in observations of the Jovian atmosphere, where the 647 nm ammonia absorption band [13] is known to be prominent. While the empirical energies in these high energy regions should be accurate, the assignment of quantum numbers to these states should be regarded with caution. A great deal of the visible ammonia spectrum remains unassigned, as well as being limited in accuracy, so there is clear scope for future experimental and computational efforts to further resolve and characterize the ammonia spectrum in these highly excited bands.

CRediT authorship contribution statement

Oleksiy A. Smola: Writing – review & editing, Writing – original draft, Visualization, Validation, Software, Methodology, Investigation, Formal analysis, Data curation, Conceptualization. **Sergei N. Yurchenko:** Writing – review & editing, Visualization, Validation, Supervision, Resources, Project administration, Methodology, Investigation, Funding acquisition, Formal analysis, Data curation, Conceptualization. **Jonathan Tennyson:** Writing – review & editing, Validation, Software, Resources, Project administration, Methodology, Funding acquisition, Formal analysis, Data curation, Conceptualization.

Declaration of competing interest

The authors declare that they have no known competing financial interests or personal relationships that could have appeared to influence the work reported in this paper.

Acknowledgments

The authors would like to thank Patrick Irwin for kindly sharing the Jupiter spectrum for comparison. JT and SY acknowledge the support of the European Research Council (ERC) under the European Union's Horizon 2020 research and innovation programme through Advance Grant number 883830. SY thanks STFC Project No. ST/Y001508/1. The authors acknowledge the use of the DiRAC Data Intensive service DIaL2.5 at the University of Leicester, managed on behalf of the STFC DiRAC HPC Facility (www.dirac.ac.uk). These DiRAC services were funded by BEIS, UKRI and STFC capital funding and STFC operations grants. DiRAC is part of the UKRI Digital Research Infrastructure.

Appendix A. Ammonia MARVEL data sets

Supplementary material related to this article can be found online at https://doi.org/10.1016/j.jqsrt.2025.109620.

Data availability

The data and a link to the repository is provided as part of the publication.

References

[1] Cheung AC, Rank DM, Townes CH, Thornton DD, Welch WJ. Detection of NH_3 molecules in the interstellar medium by their microwave emission. Phys Rev Lett 1968;21:1701–5. http://dx.doi.org/10.1103/PhysRevLett.21.1701.

[2] Ho PTP, Townes CH. Interstellar ammonia. Annu Rev Astron Astrophys 1983;21:239–70. http://dx.doi.org/10.1146/annurev.aa.21.090183.001323.

[3] Walmsley CM. Ammonia in the interstellar medium. In: AIP conference proceedings. vol. 312, Mont Sainte-Odile, France: AIP; 1994, p. 463–75. http://dx.doi.org/10.1063/1.46570.

[4] Saumon D, Marley MS, Cushing MC, Leggett SK, Roellig TL, Lodders K, Freedman RS. Ammonia as a tracer of chemical equilibrium in the T7. 5 dwarf Gliese 570D. Astrophys J 2006;647:552. http://dx.doi.org/10.1086/505419.

[5] Ott J, Henkel C, Braatz JA, Weiß A. Ammonia as a temperature tracer in the ultraluminous galaxy merger arp 220. Astrophys J 2011;742:95. http://dx.doi.org/10.1088/0004-637X/742/2/95.

[6] Juvela M, Harju J, Ysard N, Lunttila T. Reliability of NH_3 as the temperature probe of cold cloud cores. Astron Astrophys 2012;538:A133. http://dx.doi.org/10.1051/0004-6361/201118257.

[7] Doherty MJ, Geach JE, Ivison RJ, Menten KM, Jacob AM, Forbrich J, Dye S. Ammonia in the interstellar medium of a star- bursting disc at z = 2.6. Mon Not R Astron Soc: Lett 2022;517:L60–4. http://dx.doi.org/10.1093/mnrasl/slac111.

[8] Woodman JH, Trafton L, Owen T. The abundances of ammonia in the atmospheres of Jupiter, Saturn, and Titan. Icarus 1977;32:314–20. http://dx.doi.org/10.1016/0019-1035(77)90004-5.

[9] Lutz BL, Owen T. Visible bands of ammonia - band strengths, curves of growth, and the spatial-distribution of ammonia on Jupiter. Astrophys J 1980;235:285–93. http://dx.doi.org/10.1086/157632.

[10] Smith WH, Macy W, Cochran W. Ammonia in the atmospheres of Saturn and Jupiter. Icarus 1980;42:93–101. http://dx.doi.org/10.1016/0019-1035(80)90247-X.

[11] Baines KH, Carlson RW, Kamp LW. Fresh ammonia ice clouds in Jupiter. Icarus 2002;159:74–94. http://dx.doi.org/10.1006/icar.2002.6901.

[12] Irwin PGJ, Bowles N, Braude AS, Garland R, Calcutt S. Analysis of gaseous ammonia (NH3) absorption in the visible spectrum of Jupiter. Icarus 2018;302:426–36. http://dx.doi.org/10.1016/j.icarus.2017.11.031.

[13] Hill SM, Irwin PGJ, Alexander C, Rogers JH. Spatial variations of jovian tropospheric ammonia via ground-based imaging. Earth Space Sci 2024;11:e2024EA003562. http://dx.doi.org/10.1029/2024EA003562.

[14] Irwin PGJ, Hill SM, Fletcher LN, Alexander C, Rogers JH. Clouds and ammonia in the atmospheres of Jupiter and Saturn determined from a band-depth analysis of VLT/MUSE Observations. J Geophys Res: Planets 2025;130:e2024JE008622. http://dx.doi.org/10.1029/2024JE008622.

[15] Malin M, Boccaletti A, Perrot C, Baudoz P, Rouan D, Lagage P-O, Waters R, Gudel M, Henning T, Vandenbussche B, Absil O, Barrado D, Charnay B, Choquet E, Cossou C, Danielski C, Decin L, Glauser AM, Pye J, Olofsson G, Glasse A, Patapis P, Royer P, Scheithauer S, Serabyn E, Tremblin P, Whiteford N, van Dishoeck EF, Ostlin G, Ray TP, Wright G. First unambiguous detection of ammonia in the atmosphere of a planetary mass companion with JWST/MIRI coronagraphs. Astron Astrophys 2025;693:A315. http://dx.doi.org/10.1051/0004-6361/202452695.

[16] MacDonald RJ, Madhusudhan N. HD 209458b in new light: evidence of nitrogen chemistry, patchy clouds and sub-solar water. Mon Not R Astron Soc 2017;469:1979–96. http://dx.doi.org/10.1093/mnras/stx804.

[17] Whiteford N, Glasse A, Chubb KL, Kitzmann D, Ray S, Phillips MW, Biller BA, Palmer P, I, Rice K, Waldmann IP, Changeat Q, Skaf N, Wang J, Edwards B, Al-Refaie A. Retrieval study of cool directly imaged exoplanet 51 Eri b. Mon Not R Astron Soc 2023;525:1375–400. http://dx.doi.org/10.1093/mnras/stad670.

[18] Huang J, Seager S, Petkowski JJ, Ranjan S, Zhan Z. Assessment of ammonia as a biosignature gas in exoplanet atmospheres. Astrobiol 2022.

[19] Lucas PW, Tinney CG, Burningham B, Leggett SK, Pinfield DJ, Smart R, Jones HRA, Marocco F, Barber RJ, Yurchenko SN, Tennyson J, Ishii M, Tamura M, Day-Jones AC, Adamson A, Allard F, Homeier D. The discovery of a very cool, very nearby brown dwarf in the galactic plane. Mon Not R Astron Soc 2010;408:L56–60.

[20] Zalesk JA, Line MR, Schneider AC, Patience J. A uniform retrieval analysis of ultra-cool dwarfs. III. Properties of Y dwarfs. Astrophys J 2019;877:24. http://dx.doi.org/10.3847/1538-4357/ab16db.

[21] Erisman JW, Sutton MA, Galloway J, Klimont Z, Winiwarter W. How a century of ammonia synthesis changed the world. Nat Geosci 2008;1:636–9. http://dx.doi.org/10.1038/ngeo325.

[22] Fowler D, Coyle M, Skiba U, Sutton MA, Cape JN, Reis S, Sheppard LJ, Jenkins A, Grizzetti B, Galloway JN, Vitousek P, Leach A, Bouwman AF, Butterbach-Bahl K, Dentener F, Stevenson D, Amann M, Voss M. The global nitrogen cycle in the twenty-first century. Phil Trans R Soc B 2013;368:20130164. http://dx.doi.org/10.1098/rstb.2013.0164.

[23] Erisman JW, Galloway JN, Seitzinger S, Bleeker A, Dise NB, Petrescu AMR, Leach AM, de Vries W. Consequences of human modification of the global nitrogen cycle. Phil. Trans R Soc B 2013;368:20130116. http://dx.doi.org/10.1098/rstb.2013.0116.

[24] Van Damme M, Clarisse L, Heald CL, Hurtmans D, Ngadi Y, Clerbaux C, Dolman AJ, Erisman JW, Coheur PF. Global distributions, time series and error characterization of atmospheric ammonia (NH_3) from IASI satellite observations. Atmos Chem Phys 2014;14:2905–22. http://dx.doi.org/10.5194/acp-14-2905-2014.

[25] Noppen L, Clarisse L, Tack F, Ruhtz T, Merlaud A, Van Damme M, Van Roozendael M, Schuettemeyer D, Coheur P. Constraining industrial ammonia emissions using hyperspectral infrared imaging. Remote Sens Environ 2023;291:113559. http://dx.doi.org/10.1016/j.rse.2023.113559.

[26] Pai SJ, Heald CL, Murphy JG. Exploring the global importance of atmospheric ammonia oxidation. ACS Earth Space Chem 2021;5:1674–85. http://dx.doi.org/10.1021/acsearthspacechem.1c00021.

[27] Tian H, Xu R, Canadell JG, Thompson RL, Winiwarter W, Suntharalingam P, Davidson EA, Ciais P, Jackson RB, Janssens-Maenhout G, Prather MJ, Regnier P, Pan N, Pan S, Peters GP, Shi H, Tubiello FN, Zaehle S, Zhou F, Arneth A, Battaglia G, Berthet S, Bopp L, Bouwman AF, Buitenhuis ET, Chang J, Chipperfield MP, Dangal SRS, Dlugokencky E, Elkins JW, Eyre BD, Fu B, Hall B, Ito A, Joos F, Krummel PB, Landolfi A, Laruelle GG, Lauerwald R, Li W, Lienert S, Maavara T, MacLeod M, Millet DB, Olin S, Patra PK, Prinn RG, Raymond PA, Ruiz DJ, Van Der Werf GR, Vuichard N, Wang J, Weiss RF, Wells KC, Wilson C, Yang J, Yao Y. A comprehensive quantification of global nitrous oxide sources and sinks. Nature 2020;586:248–56. http://dx.doi.org/10.1038/s41586-020-2780-0.

[28] Ames JS. The spectrum researches OP Professor J.M. Eder and E. Valenta. Astrophys J 1895;1:443. http://dx.doi.org/10.1086/140084.

[29] Rimmer WB. The spectrum of ammonia. Proc R Soc Lond Ser A 1923;103:696–705. http://dx.doi.org/10.1098/rspa.1923.0089.

[30] Dennison DM, Hardy JD. The parallel type absorption bands of ammonia. Phys Rev 1932;39:938–47. http://dx.doi.org/10.1103/PhysRev.39.938.

[31] Wright N, Randall HM. The far infrared absorption spectra of ammonia and phosphine gases under high resolving power. Phys Rev 1933;44:391–8. http://dx.doi.org/10.1103/PhysRev.44.391.

[32] Cleeton CE, Williams NH. Electromagnetic waves of 1.1 cm wave-length and the absorption spectrum of ammonia. Phys Rev 1934;45:234–7. http://dx.doi.org/10.1103/PhysRev.45.234.

[33] Gordon JP, Zeiger HJ, Townes CH. The maser—new type of microwave amplifier, frequency standard, and spectrometer. Phys Rev 1955;99:1264–74. http://dx.doi.org/10.1103/PhysRev.99.1264, URL: https://link.aps.org/doi/10.1103/PhysRev.99.1264.

[34] Handy NC, Carter S, Colwell SM. The vibrational energy levels of ammonia. Mol Phys 1999;96:477–91. http://dx.doi.org/10.1080/00268979909482985.

[35] Rajamäki T, Miani A, Pesonen J, Halonen L. Six-dimensional variational calculations for vibrational energy levels of ammonia and its isotopomers. Chem Phys Lett 2002;363:226–32. http://dx.doi.org/10.1016/S0009-2614(02)01137-5.

[36] Léonard C, Handy NC, Carter S, Bowman JM. The vibrational levels of ammonia. Spectrochim Acta A 2002;58:825–38. http://dx.doi.org/10.1016/S1386-1425(01)00671-0.

[37] Colwell SM, Carter S, Handy NC. The rovibrational levels of ammonia. Mol Phys 2003;101:523–44. http://dx.doi.org/10.1080/00268970210159451.

[38] Rajamäki T, Miani A, Halonen L. Vibrational energy levels for symmetric and asymmetric isotopomers of ammonia with an exact kinetic energy operator and new potential energy surfaces. J Chem Phys 2003;118:6358–69. http://dx.doi.org/10.1063/1.1555801.

[39] Yurchenko SN, Barber RJ, Tennyson J. A variationally computed hot line list for NH_3. Mon Not R Astron Soc 2011;413:1828–34. http://dx.doi.org/10.1111/j.1365-2966.2011.18261.x.

[40] Polyansky OL, Ovsyannikov RI, Kyuberis AA, Lodi L, Tennyson J, Yachmenev A, Yurchenko SN, Zobov NF. Calculation of rotation-vibration energy levels of the ammonia molecule based on an ab initio potential energy surface. J Mol Spectrosc 2016;327:21–30. http://dx.doi.org/10.1016/j.jms.2016.08.003.

[41] Egorov O, Rey M, Nikitin A, V, Viglaska D. New Ab initio potential energy surfaces for NH3 constructed from explicitly correlated coupled-cluster methods. J Phys Chem A 2022. http://dx.doi.org/10.1021/acs.jpca.1c08717.

[42] Furtenbacher T, Coles PA, Tennyson J, Yurchenko SN, Yu S, Drouin B, Tóbiás R, Császár AG. Empirical rovibational energy of ammonia up to 7500 cm^{-1}. J Quant Spectrosc Radiat Transfer 2020;251:107027. http://dx.doi.org/10.1016/j.jqsrt.2020.107027.

[43] Furtenbacher T, Császár AG, Tennyson J. MARVEL: measured active rotational-vibrational energy levels. J Mol Spectrosc 2007;245:115–25. http://dx.doi.org/10.1016/j.jms.2007.07.005.

[44] Coles PA, Yurchenko SN, Tennyson J. ExoMol molecular line lists XXXV: a rotation-vibration line list for hot ammonia. Mon Not R Astron Soc 2019;490:4638–47. http://dx.doi.org/10.1093/mnras/stz2778.

[45] McKemmish LK, Masseron T, Sheppard S, Sandeman E, Schofield Z, Furtenbacher T, Császár AG, Tennyson J, Sousa-Silva C. MARVEL analysis of the measured high-resolution spectra of $^{48}Ti^{16}O$. Astrophys J Suppl Ser 2017;228:15. http://dx.doi.org/10.3847/1538-4365/228/2/15.

[46] McKemmish LK, Borsovszky J, Goodhew KL, Sheppard S, Bennett AFV, Martin ADJ, Singh A, Sturgeon CAJ, Furtenbacher T, Császár AG, Tennyson J. Marvel analysis of the measured high-resolution rovibronic spectra of $^{90}Zr^{16}O$. Astrophys J 2018;867:33. http://dx.doi.org/10.3847/1538-4357/aadd19.

[47] Darby-Lewis D, Shah H, Joshi D, Khan F, Kauwo M, Sethi N, Bernath PF, Furtenbacher T, T'obi'as R, Császár AG, Tennyson J. MARVEL analysis of the measured high-resolution spectra of ^{14}NH. J Mol Spectrosc 2019;362:69–76. http://dx.doi.org/10.1016/j.jms.2019.06.002.

[48] Bowesman CA, Akbari H, Hopkins S, Yurchenko SN, Tennyson J. Fine and hyperfine resolved empirical energy levels for VO. J Quant Spectrosc Radiat Transfer 2022;289:108295. http://dx.doi.org/10.1016/j.jqsrt.2022.108295.

[49] Brady RP, Yurchenko SN, Tennyson J, Kim G-S. Exomol line lists – LVI. the SO line list, MARVEL analysis of experimental transition data and refinement of the spectroscopic model. Mon Not R Astron Soc 2024;527:6675–90. http://dx.doi.org/10.1093/mnras/stad3508.

[50] Chubb KL, Joseph M, Franklin J, Choudhury N, Furtenbacher T, Császár AG, Gaspard G, Oguoko P, Kelly A, Yurchenko SN, Tennyson J, Sousa-Silva C. MARVEL analysis of the measured high-resolution spectra of C_2H_2. J Quant Spectrosc Radiat Transfer 2018;204:42–55. http://dx.doi.org/10.1016/j.jqsrt.2017.08.018.

[51] Chubb KL, Naumenko OV, Keely S, Bartolotto S, MacDonald S, Mukhtar M, Grachov A, White J, Coleman E, Hu S-M, Liu A, Fazliev AZ, Polovtseva ER, Horneman VM, Campargue A, Furtenbacher T, Császár AG, Yurchenko SN, Tennyson J. MARVEL analysis of the measured high-resolution rovibrational spectra of H_2S. J Quant Spectrosc Radiat Transfer 2018;218:178–86. http://dx.doi.org/10.1016/j.jqsrt.2018.07.012.

[52] Al-Derzi AR, Yurchenko SN, Tennyson J, Melosso M, Jiang N, Puzzarini C, Dore L, Furtenbacher T, Tobias R, Császár AG. An improved rovibrational linelist of formaldehyde, $H_2{}^{12}C^{16}O$. J Quant Spectrosc Radiat Transfer 2021;266:107563. http://dx.doi.org/10.1016/j.jqsrt.2021.107563.

[53] Mellor T, Owens A, Yurchenko SN, Tennyson J. MARVEL analysis of high-resolution spectra of thioformaldehyde (H_2CS). J Mol Spectrosc 2023;391:111732. http://dx.doi.org/10.1016/j.jms.2022.111732.

[54] Kefala K, Boudon V, Yurchenko SN, Tennyson J. Empirical rovibrational energy levels for methane. J Quant Spectrosc Radiat Transfer 2024;316:108897. http://dx.doi.org/10.1016/j.jqsrt.2024.108897.

[55] Upadhyay A, Furtenbacher T, Conway EK, Bowesman CA, Dobney CP, Bowen E, Broner D, Ciobanu V, Gelborova K, Livsey S, Magbagbeola D, Manjunatha M, Mitchell T, Morohunfola D, Wijayakoon E, Winter S, Chubb KL, Tennyson J. MARVEL analysis of measured high-resolution rovibrational spectra of ($^{16}o_3$). J Quant Spectrosc Radiat Transfer 2025;338:109399. http://dx.doi.org/10.1016/j.jqsrt.2025.109399.

[56] Al Derzi AR, Furtenbacher T, Yurchenko SN, Tennyson J, Császár AG. MARVEL analysis of the measured high-resolution spectra of $^{14}NH_3$. J Quant Spectrosc Radiat Transfer 2015;161:117–30. http://dx.doi.org/10.1016/j.jqsrt.2015.03.034.

[57] Cazzoli G, Dore L, Puzzarini C. The hyperfine structure of the inversion-rotation transition $J_K = 1_0 \leftarrow 0_0$ of NH_3 investigated by lamb-dip spectroscopy. Astron Astrophys 2009;507:1707–10.

[58] Kukolich SG, Wofsy SC.$^{14}nh_3$ hyperfine structure and quadrupole coupling. J Chem Phys 1970;52:5477–81.

[59] Kukolich SG. Measurement of ammonia hyperfine structure with a two-cavity maser. Phys Rev 1967;156:83–92.

[60] Kukolich SG. Measurement of hyperfine structure of the J = 3, K = 2 inversion line of $N^{14}H_3$. Phys Rev 1965;138:A1322–5. http://dx.doi.org/10.1103/PhysRev.138.A1322.

[61] Poynter RL, Kakar RK. The microwave frequencies, line parameters, and spectral constants for $^{14}nh_3$. Astrophys J Suppl Ser 1975;29:87–96.

[62] Cohen EA, Poynter RL. The microwave spectrum of $^{14}NH_3$ in the υ = 000011 state. J Mol Spectrosc 1974;53:131–9.

[63] Sinha BV, Smith PDP. New microwave inversion lines of $14NH_3$ in the ground state. J Mol Spectrosc 1980;80:231–2.

[64] Coy SL, Lehmann KK. Rotational structure of ammonia N-H stretch overtones: Five and six quanta bands. J Chem Phys 1986;84:5239–49.

[65] Sasada H, Hasegawa Y, Amano T, Shimizu T. High-resolution infrared and microwave spectroscopy of the ν_4 and $2\nu_2$ bands of $^{14}NH_3$ and $^{15}NH_3$. J Mol Spectrosc 1982;96:106–30.

[66] Winnewisser G, Belov SP, Klaus T, Urban S. Ro-inversional spectrum of ammonia. Z Naturforsch 1996;51:200–6.

[67] Twagirayezu S, Hall GE, Sears TJ. Quadrupole splittings in the near-infrared spectrum of $^{14}NH_3$. J Chem Phys 2016;145:144302.

[68] Fichoux H, Khelkhal M, Rusinek E, Legrand J, Herlemont F, Urban Š. Double resonance sub-Doppler study of the allowed and $\Delta K = -3$ forbidden $Q(3,3)$ transitions to the ν_2 vibrational state of $^{14}NH_3$. J Mol Spectrosc 1998;192:169–78.

[69] Tanaka K, Endo Y, Hirota E. Submillimeter-wave spectrum of $k = \pm 1 \leftarrow \mp 2$ transitions of NH_3. Chem Phys Lett 1988;146:165–8.

[70] Smith PDP, firth S, Davis RW. High J inversion lines of ammonia. J Mol Spectrosc 1990;144:448–50.

[71] Sasada H, Endo Y, Hirota E, Poynter RL, Margolis JS. Microwave and fourier-transform infrared spectroscopy of the $\upsilon_4 = 1$ and $\upsilon_2 = 2$ states of NH_3. J Mol Spectrosc 1992;151:33–53.

[72] Cohen EA. The ν_4 state inversion spectra of $^{15}NH_3$ and $^{14}NH_3$. J Mol Spectrosc 1980;79:496–501.

[73] Drouin BJ, Yu S, Pearson JC, Gupta H. Terahertz spectroscopy for space applications: 2.5–2.7 THz spectra of HD, H_2O and NH_3. J Mol Struct 2011;1006:2–12.

[74] Lemarchand C, Triki M, Darquie B, Borde CJ, Chardonnet C, Daussy C. Progress towards an accurate determination of the Boltzmann constant by Doppler spectroscopy. New J Phys 2011;13:073028. http://dx.doi.org/10.1088/1367-2630/13/7/073028.

[75] Yu S, Pearson JC, Drouin BJ, Sung K, Pirali O, Vervloet M, Martin-Drumel M-A, Endres CP, Shiraishi T, Kobayashi K, Matsushima F. Submillimeter-wave and far-infrared spectroscopy of high-j transitions of the ground and $\upsilon_2 = 1$ states of ammonia. J Chem Phys 2010;133:174317.

[76] Sun Z-D, Lees R, Xu L-H. Lamb-dip measurements of ammonia calibration lines in methylamine using a dual-mode CO_2-laser-microwave-sideband spectrometer. J Mol Spectrosc 2008;249:68–70. http://dx.doi.org/10.1016/j.jms.2008.02.001.

[77] Magerl G, Schupita W, Frye JM, Kreiner WA, Oka T. Sub-doppler spectroscopy of the ν_2 band of NH_3 using microwave modulation sidebands of CO_2 laser lines. J Mol Spectrosc 1984;107:72–83. http://dx.doi.org/10.1016/0022-2852(84)90266-2.

[78] Krupnov AF, Tretyakov MY, Bogey M, Bailleux S, Walters A, Delcroix B, Civiš S. Microwave measurements of $J = 2 \leftarrow 1, K = 0, 1$ ammonia transitions at 1.215 THz. J Mol Spectrosc 1996;176:442–3.

[79] Pearson JC, Yu S, Pirali O. Modeling the spectrum of the $2\upsilon_2$ and υ_4 states of ammonia to experimental accuracy. J Chem Phys 2016;145:124301.

[80] Chen P, Pearson JC, Pickett HM, Matsuura S, Blake GA. Measurements of $^{14}NH_3$ in the state by a solid-state, photomixing, THz spectrometer, and a simultaneous analysis of the microwave, terahertz, and infrared transitions between the ground and inversion-rotation levels. J Mol Spectrosc 2006;236:116–26.

[81] Urban Š, Herlemont F, Khelkhal M, Fichoux H, Legrand J. High-accuracy determination of the frequency and quadrupole structure of the $sP(1,\,0)$ and $aR(0,\,0)$ transitions to the ν_2 state of $^{14}NH_3$. J Mol Spectrosc 2000;200:280–2. http://dx.doi.org/10.1006/jmsp.1999.8042.

[82] Belov SP, Urban Š, Winnewisser G. Hyperfine structure of rotation-inversion levels in the excited ν_2 state of ammonia. J Mol Spectrosc 1998;189:1–7.

[83] Siemsen KJ, Reid J. Heterodyne frequency measurements of $^{14}NH_3$ and $^{15}nh_3$ υ_2-band transitions. Opt Lett 1985;10:594–6.

[84] Belov SP, Gershstein LI, Krupnov AF, Maslovskij AV, Urban Š, Špirko V, Papousek D. Inversion and inversion-rotation spectrum of $^{14}NH_3$ in the ν_2 excited state. J Mol Spectrosc 1980;84:288–304.

[85] Guinet M, Jeseck P, Mondelain D, Pepin I, Janssen C, Camy-Peyret C, Mandin JY. Absolute measurements of intensities, positions and self-broadening coefficients of R branch transitions in the ν_2 band of ammonia. J Quant Spectrosc Radiat Transfer 2011;112:1950–60.

[86] Minguzzi P, Tonelli M, Carrozzi A, Di Lieto A. Optoacoustic laser Stark spectroscopy in the ν_2 band of $^{14}NH_3$. J Mol Spectrosc 1982;96:294–305. http://dx.doi.org/10.1016/0022-2852(82)90193-X.

[87] Brown LR, Toth RA. Comparison of the frequencies of NH_3, CO_2, H_2O, N_2O, CO, and CH_4 as infrared calibration standards. J Opt Soc Am B 1985;2:842–56.

[88] Sasada H, Schwendeman RH, Magerl G. High-resolution spectroscopy of the $\upsilon_2 = 2$ a $\leftarrow \upsilon_2 = 1$ s band of $14NH_3$. J Mol Spectrosc 1986;117:317–30.

[89] Urban Š, Tu N, Narahari Rao K, Guelachvili G. Analysis of high-resolution Fourier transform spectra of $^{14}NH_3$ at 2.3 μm. J Mol Spectrosc 1989;133:312–30.

[90] Kostiuk T, Mumma MJ, Hillman JJ, Buhl D, Brown LW, Faris JL. NH_3 spectral line measurements on earth and jupiter using 10 mm superheterodyne receiver. Infrared Phys 1977;17:431–9.

[91] Sattler JP, Worchesky TL. Additional diode laser heterodyne measurements on ammonia. J Mol Spectrosc 1981;90:297–301.

[92] Chu Z, Chen L, Cheo PK. Absorption spectra of NH_3 using a microwave-sideband CO_2-laser spectrometer. J Quant Spectrosc Radiat Transfer 1994;51:591–602.

[93] Shoja-Chaghervand P, Bjarnov E, Schwendeman R. Infrared-microwave two-photon spectroscopy of the ν_2 band of $^{14}NH_3$. J Mol Spectrosc 1983;97:287–305. http://dx.doi.org/10.1016/0022-2852(83)90268-0.

[94] Poynter RL, Margolis JS. The ground state far infrared spectrum of NH_3. Mol Phys 1983;48:401–18.

[95] Poynter RL, Margolis JS. The ν_2 spectrum of nh_3. Mol Phys 1984;51:393–412.

[96] Urban Š, Papoušek D, Kauppinen J, Yamada K, Winnewisser G. The ν_2 band of $^{14}NH_3$: A calibration standard with better than 1×10^{-4} cm^{-1} precision. J Mol Spectrosc 1983;101:1–15.

[97] Hillman JJ, Jennings DE, Faris JL. Diode laser–CO_2 laser heterodyne spectrometer: measurement of 2sQ(1), 1) in $2\nu_2 - \nu_2$ of NH_3. Appl Opt 1979;18:1808–11.

[98] Fabian M, Ito F, Yamada KMT. N_2, O_2, and air broadening of NH_3 in υ_2 band measured by ftir spectroscopy. J Mol Spectrosc 1995;173:591–602.

[99] Sattler JP, Miller LS, Worchesky TL. Diode laser heterodyne measurements on $^{14}NH_3$. J Mol Spectrosc 1981;88:347–51.

[100] Hillman JJ, Kostiuk T, Buhl D, Faris JL, Novaco JC, Mumma MJ. Precision measurements of NH_3 spectral lines near 11 μm using the infrared heterodyne technique. Opt Lett 1977;1:81. http://dx.doi.org/10.1364/OL.1.000081.

[101] Cottaz C, Kleiner I, Tarrago G, Brown LR, Margolis JS, Poynter RL, Pickett HM, Fouchet T, Drossart P, Lellouch E. Line positions and intensities in the $2\nu_2/\nu_4$ vibrational system of $^{14}NH_3$ near 5–7 μm. J Mol Spectrosc 2000;203:285–309.

[102] Aroui H, BenMabrouk K. Line-mixing effect on NH_3 line intensities. J Quant Spectrosc Radiat Transfer 2013;130:273–83.

[103] Freund SM, Oka T. Infrared-microwave two-photon spectroscopy: The ν_2 band of NH_3. Phys Rev A 1976;13:2178–90.

[104] Brown LR, Margolis JS. Empirical line parameters of NH_3 from 4791 to 5294 cm^{-1}. J Quant Spectrosc Radiat Transfer 1996;56:283–94.

[105] Fabian M, Yamada KMT. Absolute intensity of the nh_3 ν_2 band. J Mol Spectrosc 1999;198:102–9.

[106] Pine AS, Dang-Nhu M. Spectral intensities in the ν_1 band of NH_3. J Quant Spectrosc Radiat Transfer 1993;50:565–70.

[107] Lellouch E, Lacome N, Guelachvili G, Tarrago G, Encrenaz T. Ammonia: Experimental absolute linestrengths and self-broadening parameters in the 1800 to 2100 cm^{-1} range. J Mol Spectrosc 1987;124:333–47.

[108] Weber WH. Laser-stark spectrum of NH_3 with the CO laser: Determination of the ground state dipole moment. J Mol Spectrosc 1984;107:405–16.

[109] Brown LR, Peterson DB. An empirical expression for linewidths of ammonia from far-infrared measurements. J Mol Spectrosc 1994;168:593–606.

[110] Urban Š, Špirko V, Papoušek D, Kauppinen J, Belov SP, Gershtein LI, Krupnov AF. A simultaneous analysis of the microwave, submillimeterwave, far infrared, and infrared-microwave two-photon transitions between the ground and ν_2 inversion-rotation levels of $^{14}NH_3$. J Mol Spectrosc 1981;88:274–92.

[111] Pearson J, Yu S, Pearson J, Sung K, Drouin B, Pirali O. Extended measurements and an experimental accuracy effective Hamiltonian model for the $3\nu_2$ and $\nu_4+\nu_2$ states of ammonia. J Mol Spectrosc 2018;353:60–6. http://dx.doi.org/10.1016/j.jms.2018.09.004.

[112] Kleiner I, Brown LR, Tarrago G, Kou Q-L, Picqué N, Guelachvili G, Dana V, Mandin J-Y. Positions and intensities in the $2\nu_4/\nu_1/\nu_3$ vibrational system of $^{14}NH_3$ near 3 μm. J Quant Spectrosc Radiat Transfer 1999;193:46–71.

[113] D'Cunha R. The $a2\nu_2 \leftarrow s\nu_2$ bands of $^{14}NH_3$ and $^{15}NH_3$. J Mol Spectrosc 1987;122:130–4.

[114] Nereson N. Diode laser measurements of NH_3 absorption lines around 10.6 μm. J Mol Spectrosc 1978;69:489–93.

[115] Papousek D, Urban S, Spirko V, Rao KN. The $\Delta k = \pm 2$ and $\Delta k = \pm 3$ forbidden transitions in the vibrational-rotational spectra of symmetric top molecules NH_3 and H_3O^+. J Mol Spectrosc 1986;141:361–6.

[116] Jones H. Infrared-microwave two-photon spectroscopy with $^{13}C^{16}o_2$ and $^{12}C^{18}O_2$ lasers of the ν_2-band of ammonia. Appl Phys 1978;15:261–4. http://dx.doi.org/10.1007/BF00896106.

[117] Sung K, Yu S, Pearson J, Pirali O, Tchana FK, Manceron L. Far-infrared $^{14}NH_3$ line positions and intensities measured with a FT-IR and AILES beamline, synchrotron SOLEIL. J Mol Spectrosc 2016;327:1–20.

[118] Cottaz C, Tarrago G, Kleiner I, Brown LR. Assignments and intensities of $^{14}NH_3$ hot bands in the 5-to 8-μm ($3\nu_2-\nu_2$, $\nu_2+\nu_4-\nu_2$) and 4-μm ($4\nu_2-\nu_2$, $\nu_1-\nu_2$, $\nu_3-\nu_2$ and $2\nu_4-\nu_2$) regions. J Mol Spectrosc 2001;209:30–49.

[119] Guelachvili G, Abdullah AH, Tu N, Narahari Rao K, Urban Š, Papoušek D. Analysis of high-resolution Fourier-transform spectra of $^{14}NH_3$ at 3.0 μm. J Mol Spectrosc 1989;133:345–64.

[120] Földes T, Golebiowski D, Herman M, Softley TP, Di Lonardo G, Fusina L. Low-temperature high-resolution absorption spectrum of $^{14}NH_3$ in the $\nu_1+\nu_3$ band region (1.51μm). Mol Phys 2014;112:2407–18.

[121] Kleiner I, Tarrago G, Brown LR. Positions and intensities in the $3\nu_2/\nu_2+\nu_4$ vibrational system of $^{14}NH_3$ near 4 μm. J Mol Spectrosc 1995;173:120–45.

[122] Cermák P, Hovorka J, Veis P, Cacciani P, Cosléou J, Romh JE, Khelkhal M. Spectroscopy of $^{14}NH_3$ and $^{15}NH_3$ in the 2.3 μm spectral range with a new VECSEL laser source. J Quant Spectrosc Radiat Transfer 2014;137:13–22.

[123] Sung K, Brown LR, Huang X, Schwenke DW, Lee TJ, Coy SL, Lehmann KK. Extended line positions, intensities, empirical lower state energies and quantum assignments of NH_3 from 6300 to 7000 cm^{-1}. J Quant Spectrosc Radiat Transfer 2012;113:1066–83. http://dx.doi.org/10.1016/j.jqsrt.2012.02.037.

[124] Urban S, D'Cunha R, Manheim J, Narahari Rao K. High-J transitions in the ν_2 bands of $^{14}NH_3$ and $^{15}NH_3$. J Mol Spectrosc 1986;118:298–309. http://dx.doi.org/10.1016/0022-2852(86)90243-2, URL: https://www.sciencedirect.com/science/article/pii/0022285286902432.

[125] Urban Š, D'Cunha R, Narahari Rao K, Papoušek D. The $\delta k = \pm 2$ "forbidden band" and inversion-rotation energy levels of ammonia. Can J Phys 1984;62:1775–91.

[126] Angstl R, Finsterholzl H, Frunder H, Illig D, Papoušek D, Pračna P, Rao KN, Schrotter HW, Urban Š. Fourier transform and CARS spectroscopy of the ν_1 and ν_3 fundamental bands of $^{14}NH_3$. J Mol Spectrosc 1985;114:454–72.

[127] Zobov NF, Shirin SV, Ovsyannikov RI, Polyansky OL, Yurchenko SN, Barber RJ, Tennyson J, Hargreaves RJ, Bernath PF. Analysis of high temperature ammonia spectra from 780 to 2100 cm^{-1}. J Mol Spectrosc 2011;269:104–8.

[128] Down MJ, Hill C, Yurchenko SN, Tennyson J, Brown LR, Kleiner I. Re-analysis of ammonia spectra: Updating the HITRAN $^{14}NH_3$ database. J Quant Spectrosc Radiat Transfer 2013;130:260–72.

[129] Hermanussen J, Bizzarri A, Baldacchini G. Diode laser measurements of ammonia absorption lines over the range 620–740 cm^{-1}. J Mol Spectrosc 1986;119:291–8.

[130] Lees RM, Li L, Xu L-H. New VISTA on ammonia in the 1.5 μm region: Assignments for the ν_3+$2\nu_4$ bands of $^{14}NH_3$ and $^{15}NH_3$ by isotopic shift labeling. J Mol Spectrosc 2008;251:241–51.

[131] Dietiker P, Milogyadov E, Quack M, Schneider A, Seyfang G. Two photon IR-laser induced population transfer in NH_3 – first steps to measure parity violation in chiral molecules. In: Stock D, Wester R, Scheier P, editors. Proceedings of the 19th symposium on atomic, cluster and surface physics 2014. SASP 2014, Insbruck: Innsbruck University Press; 2014.

[132] Li L, Lees RM, Xu L-H. External cavity tunable diode laser spectra of the $\nu_1+2\nu_4$ stretch-band combination bands of $^{14}NH_3$ and $^{15}NH_3$. J Mol Spectrosc 2007;243:219–26.

[133] Snels M, Baldacchini G. Shape and width of IR absorption lines of ammonia expanded in a supersonic jet. Appl Phys B 1988;47:277–82.

[134] Helminger P, De Lucia FC, Gordy W. Rotational spectra of NH_3 and ND_3 in the 0.5-mm wavelength region. J Mol Spectrosc 1971;39:94–7.

[135] Urban Š, Misra P, Narahari Rao K. The $\nu_1+\nu_2$ and $\nu_1+\nu_2-\nu_2$ bands of $^{14}NH_3$ and $^{15}NH_3$. J Mol Spectrosc 1985;114:377–94.

[136] Petersen JC, Hald J. Microwave optical double resonance spectroscopy of ammonia in a hollow-core fiber. Opt Express 2010;vol. 18:7955–64.

[137] Lundsberg-Nielsen L, Hegelund F, Nicolaisen FM. Analysis of the high-resolution spectrum of ammonia ($^{14}NH_3$) in the near-infrared region, 6400–6900 cm^{-1}. J Mol Spectrosc 1993;162:230–45.

[138] Berden G, Peeters R, Meijer G. Cavity-enhanced absorption spectroscopy of the 1.5 μm band system of jet-cooled ammonia. Chem Phys Lett 1999;307:131–8.

[139] Urban Š, Špirko V, Papoušek D, McDowell RS, Nereson NG, Belov SP, Gershstein LI, Maslovskij AV, Krupnov AF, Curtis J, Narahari Rao K. Coriolis and l-type interactions in the ν_2, $2\nu_2$, and ν_4 states of $^{14}NH_3$. J Mol Spectrosc 1980;79:455–95.

[140] Barton EJ, Yurchenko SN, Tennyson J, Clausen S, Fateev A. High-resolution absorption measurements of NH_3 at high temperatures: 500-2100 cm^{-1}. J Quant Spectrosc Radiat Transfer 2015;167:126–34.

[141] Yurchenko SN, Bowesman CA, Brady RP, Guest ER, Kefala K, Mitev GB, Owens A, Perri AN, Pezzella M, Smola O, Solokov A, Zhang J, Tennyson J. ExoMol line lists – LX: Molecular line list for the ammonia isotopologue $^{15}NH_3$. Mon Not R Astron Soc 2024;533:3442–56. http://dx.doi.org/10.1093/mnras/stae1849.

[142] Barton EJ, Yurchenko SN, Tennyson J, Béguier S, Campargue A. A near infrared line list for NH_3: Analysis of a kitt peak spectrum after 35 years. J Mol Spectrosc 2016;325:7–12. http://dx.doi.org/10.1016/j.jms.2016.05.001.

[143] Barton EJ, Polyansky OL, Yurchenko SN, Tennyson J, Civis S, Ferus M, Hargreaves R, Ovsyannikov I, Kyuberis AA, Zobov NF, Béguier S, Campargue A. Absorption spectra of ammonia near 1 μm. J Quant Spectrosc Radiat Transfer 2017;203:392–7. http://dx.doi.org/10.1016/j.jqsrt.2017.03.042.

[144] Zobov NF, Coles PA, Ovsyannikov RI, Kyuberis AA, Hargreaves RJ, Bernath PF, Yurchenko SN, Tennyson J, Polyansky OL. Analysis of the red and green optical absorption spectrum of gas phase ammonia. J Quant Spectrosc Radiat Transfer 2018;224–231:209. http://dx.doi.org/10.1016/j.jqsrt.2018.02.001.

[145] Maithani S, Mandal S, Maity A, Pal M, Pradhan M. High-resolution spectral analysis of ammonia near 6.2 μm using a cw EC-QCL coupled with cavity ring-down spectroscopy. Analyst 2018;143:2109–14. http://dx.doi.org/10.1039/C7AN02008B.

[146] Svoboda V, Rakovský J, Votava O. New insight on ammonia 1.5 μm overtone spectra from two-temperature analysis in supersonic jet. J Quant Spectrosc Radiat Transfer 2019;227:201–10. http://dx.doi.org/10.1016/j.jqsrt.2019.01.030.

[147] Zobov N, Bertin T, Vander Auwera J, Civiš S, Knížek A, Ferus M, Ovsyannikov RI, Makhnev VY, Tennyson J, Polyansky OL. The spectrum of ammonia near 0.793 μm. J Quant Spectrosc Radiat Transfer 2021;273:107838. http://dx.doi.org/10.1016/j.jqsrt.2021.107838.

[148] Čermák P, Cacciani P, Cosléou J. Accurate $^{14}NH_3$ line-list for the 2.3 μm spectral region. J Quant Spectrosc Radiat Transfer 2021;274:107861. http://dx.doi.org/10.1016/j.jqsrt.2021.107861.

[149] Cacciani P, Črmák P, Béguier S, Campargue A. The absorption spectrum of ammonia between 5650 and 6350 cm^{-1}. J Quant Spectrosc Radiat Transfer 2021;258:107334. http://dx.doi.org/10.1016/j.jqsrt.2020.107334.

[150] Huang X, Sung K, Toon GC, Schwenke DW, Lee TJ. A collaborative $^{14}NH_3$ IR spectroscopic analysis at 6000 cm^{-1}. J Quant Spectrosc Radiat Transfer 2022;280:108076. http://dx.doi.org/10.1016/j.jqsrt.2022.108076.

[151] Cacciani P, Cermak P, Vander Auwera J, Campargue A. The ammonia absorption spectrum between 3900 and 4700 cm^{-1}. J Quant Spectrosc Radiat Transfer 2022;277:107961. http://dx.doi.org/10.1016/j.jqsrt.2021.107961.

[152] Cacciani P, Čermák P, Vander Auwera J, Campargue A. The ammonia absorption spectrum between 4700 and 5650 cm^{-1}. J Quant Spectrosc Radiat Transfer 2022;292:108350. http://dx.doi.org/10.1016/j.jqsrt.2022.108350.

[153] Cacciani P, Cermak P, Votava O, Auwera JV, Campargue A. The ammonia absorption spectrum revisited between 5650 and 6350 cm^{-1}. Mol Phys 2023. http://dx.doi.org/10.1080/00268976.2023.2256893.

[154] Yang G, de Oliveira VS, Laumer D, Heyl CM, Yachmenev A, Hartl I, Küpper J. Self-broadening and self-shift in the $3\nu_2$ band of ammonia from mid-infrared-frequency-comb spectroscopy. J Mol Spectrosc 2023;392:111744. http://dx.doi.org/10.1016/j.jms.2023.111744.

[155] Zhu D, Agarwal S, Seifert L, Shu B, Fernandes R, Qu Z. NH_3 absorption line study and application near 1084.6 cm^{-1}. Infrared Phys Technol 2024;136:105058. http://dx.doi.org/10.1016/j.infrared.2023.105058, URL: https://www.sciencedirect.com/science/article/pii/{S1350449523005169}.

[156] Tobias R, Furtenbacher T, Simko I, Császár AG, Diouf ML, Cozijn FMJ, Staa JMA, Salumbides EJ, Ubachs W. Spectroscopic-network-assisted precision spectroscopy and its application to water. Nat Comms 2020;11:1708. http://dx.doi.org/10.1038/s41467-020-15430-6.

[157] Arendas P, Furtenbacher T, Császár AG. From bridges to cycles in spectroscopic networks. Sci Rep 2020;10:19489. http://dx.doi.org/10.1038/s41598-020-75087-5.

[158] Arendas P, Furtenbacher T, Császár AG. Verification labels for rovibronic quantum-state energy uncertainties. Sci Rep 2024;14:794. http://dx.doi.org/10.1038/s41598-023-46665-0.

[159] Tennyson J, Furtenbacher T, Yurchenko SN, Császár AG. Empirical rovibrational energy levels for nitrous oxide. J Quant Spectrosc Radiat Transfer 2024;316:108902. http://dx.doi.org/10.1016/j.jqsrt.2024.108902.

[160] Bunker PR, Jensen P. Molecular symmetry and spectroscopy. 2nd ed.. Ottawa: NRC Research Press; 1998.

[161] Down MJ, Hill C, Yurchenko SN, Tennyson J, Brown LR, Kleiner I. Re-analysis of ammonia spectra: Updating the HITRAN $^{14}NH_3$ database. J Quant Spectrosc Radiat Transfer 2013;130:260–72. http://dx.doi.org/10.1016/j.jqsrt.2013.05.027.

[162] Yurchenko SN, Thiel W, Jensen P. Theoretical rovibrational energies (TROVE): A robust numerical approach to the calculation of rovibrational energies for polyatomic molecules. J Mol Spectrosc 2007;245:126–40. http://dx.doi.org/10.1016/j.jms.2007.07.009.

[163] Beale CA, Wong A, Bernath P. Infrared transmission spectra of hot ammonia in the 4800-9000 $cm^{-1\ region}$. J Quant Spectrosc Radiat Transfer 2020;246:106911. http://dx.doi.org/10.1016/j.jqsrt.2020.106911.

[164] Vander Auwera J, Vanfleteren T. Line positions and intensities in the 7400-8600 $cm^{-1\ region\ of\ the\ ammonia\ spectrum}$. Mol Phys 2018;116:3621–30. http://dx.doi.org/10.1080/00268976.2018.1467054.

[165] Gordon IE, Rothman LS, Hill C, Kochanov RV, Tan Y, Bernath PF, Birk M, Boudon V, Campargue A, Chance KV, Drouin BJ, Flaud J-M, Gamache RR, Hodges JT, Jacquemart D, Perevalov VI, Perrin A, Shine KP, Smith M-AH, Tennyson J, Toon GC, Tran H, Tyuterev VG, Barbe A, Császár AG, Devi VM, Furtenbacher T, Harrison JJ, Hartmann J-M, Jolly A, Johnson TJ, Karman T, Kleiner I, Kyuberis AA, Loos J, Lyulin OM, Massie ST, Mikhailenko SN, Moazzen-Ahmadi N, Müller HSP, Naumenko OV, Nikitin AV, Polyansky OL, Rey M, Rotger M, Sharpe SW, Sung K, Starikova E, Tashkun SA, Vander Auwera J, Wagner G, Wilzewski J, Wcisło P, Yu S, Zak EJ. The *HITRAN* 2016 molecular spectroscopic database. J Quant Spectrosc Radiat Transfer 2016;203(2017):3–69. http://dx.doi.org/10.1016/j.jqsrt.2017.06.038.

[166] Gordon IE, et al. The HITRAN2020 molecular spectroscopic database. J Quant Spectrosc Radiat Transfer 2020;277(2022):107949. http://dx.doi.org/10.1016/j.jqsrt.2021.107949.

[167] Tennyson J, Yurchenko SN. High accuracy molecular line lists for studies of exoplanets and other hot atmospheres. Front Astron Space Sci 2022;8:795040. http://dx.doi.org/10.3389/fspas.2021.795040.

[168] Zhang J, Hill C, Tennyson J, Yurchenko SN. ExoMolHR: A relational database of empirical high-resolution molecular spectra. Astrophys J Suppl Ser 2025;276:67. http://dx.doi.org/10.3847/1538-4365/ada288.

[169] Yurchenko SN, Al-Refaie AF, Tennyson J. ExoCross: A general program for generating spectra from molecular line lists. Astron Astrophys 2018;614:A131. http://dx.doi.org/10.1051/0004-6361/201732531.

[170] Gordon IE, Rothman LS, Hargreaves RJ, Hashemi R, Karlovets EV, Skinner FM, Conway EK, Hill C, Kochanov RV, Tan Y, Wcisło P, Finenko AA, Nelson K, Bernath PF, Birk M, Boudon V, Campargue A, Chance KV, Coustenis A, Drouin BJ, Flaud J-M, Gamache RR, Hodges JT, Jacquemart D, Mlawer EJ, Nikitin AV, Perevalov VI, Rotger M, Tennyson J, Toon GC, Tran H, Tyuterev VG, Adkins EM, Baker A, Barbe A, Canè E, Császár AG, Dudaryonok A, Egorov O, Fleisher AJ, Fleurbaey H, Foltynowicz A, Furtenbacher T, Harrison JJ, Hartmann J-M, Horneman V-M, Huang X, Karman T, Karns J, Kassi S, Kleiner I, Kofman V, Kwabia-Tchana F, Lavrentieva NN, Lee TJ, Long DA, Lukashevskaya AA, Lyulin OM, Makhnev VY, Matt W, Massie ST, Melosso M, Mikhailenko SN, Mondelain D, Müller HSP, Naumenko OV, Perrin A, Polyansky OL, Raddaoui E, Raston PL, Reed ZD, Rey M, Richard C, Tóbiás R, Sadiek I, Schwenke DW, Starikova E, Sung K, Tamassia F, Tashkun SA, Vander Auwera J, Vasilenko IA, Vigasin AA, Villanueva GL, Vispoel B, Wagner G, Yachmenev A, Yurchenko SN. The HITRAN2020 molecular spectroscopic database. J Quant Spectrosc Radiat Transfer 2020;277(2022):107949. http://dx.doi.org/10.1016/j.jqsrt.2021.107949.

[171] Giver LP, Miller JH, Boese RW. A laboratory atlas of the $5\nu_1$ NH3 absorption band at 6475 åwith applications to jupiter and saturn. Icarus 1975;25:34–48. http://dx.doi.org/10.1016/0019-1035(75)90187-6.

[172] Irwin PGJ, Bowles N, Braude AS, Garland R, Calcutt S, Coles PA, Yurchenko SN, Tennyson J. Analysis of gaseous ammonia (NH_3) absorption in the visible spectrum of Jupiter - update. Icarus 2019;321:572–82. http://dx.doi.org/10.1016/j.icarus.2018.12.008.

[173] Tennyson J, Yurchenko SN. ExoMol: molecular line lists for exoplanet and other atmospheres. Mon Not R Astron Soc 2012;425:21–33. http://dx.doi.org/10.1111/j.1365-2966.2012.21440.x.

[174] Tennyson J, Yurchenko SN, Al-Refaie AF, Barton EJ, Chubb KL, Coles PA, Diamantopoulou S, Gorman MN, Hill C, Lam AZ, Lodi L, McKemmish LK, Na Y, Owens A, Polyansky OL, Rivlin T, Sousa-Silva C, Underwood DS, Yachmenev A, Zak E. The ExoMol database: molecular line lists for exoplanet and other hot atmospheres. J Mol Spectrosc 2016;327:73–94. http://dx.doi.org/10.1016/j.jms.2016.05.002.

[175] Tennyson J, Yurchenko SN, Al-Refaie AF, Clark VHJ, Chubb KL, Conway EK, Dewan A, Gorman MN, Hill C, Lynas-Gray AE, Mellor T, McKemmish LK, Owens A, Polyansky OL, Semenov M, Somogyi W, Tinetti G, Upadhyay A, Waldmann I, Wang Y, Wright S, Yurchenko OP. The release of the ExoMol database: Molecular line lists for exoplanet and other hot atmospheres. J Quant Spectrosc Radiat Transfer 2020;255:107228. http://dx.doi.org/10.1016/j.jqsrt.2020.107228.

[176] Tennyson J, Yurchenko SN, Zhang J, Bowesman CA, Brady RP, Buldyreva J, Chubb KL, Gamache RR, Gorman MN, Guest ER, Hill C, Kefala K, Lynas-Gray AE, Mellor TM, McKemmish LK, Mitev GB, Mizus II, Owens A, Peng Z, Perri AN, Pezzella M, Polyansky OL, Qu Q, Semenov M, Smola O, Solokov A, Somogyi W, Upadhyay A, Wright SOM, Zobov NF. The release of the ExoMol database: molecular line lists for exoplanet and other hot atmospheres. J Quant Spectrosc Radiat Transfer 2024;326(2024):109083. http://dx.doi.org/10.1016/j.jqsrt.2024.109083.